Open Ceramics 15 (2023) 100389

Contents lists available at ScienceDirect

Open Ceramics

journal homepage: www.sciencedirect.com/journal/open-ceramics

The use of bundles with higher filament count for cost reduction of high-strength oxide ceramic composites

Renato S.M. Almeida [a,**], Maroof A. Hoque [a], Walter E.C. Pritzkow [b], Kamen Tushtev [a,*], Kurosch Rezwan [a,c]

[a] Advanced Ceramics, University of Bremen, Bremen, 28359, Germany
[b] Walter E. C. Pritzkow Spezialkeramik, Filderstadt, 70794, Germany
[c] MAPEX - Center for Materials and Processes, University of Bremen, Bremen, 28359, Germany

ARTICLE INFO

Handling Editor: Dr P Colombo

Keywords:
All-oxide ceramic matrix composite
Nextel™ 610
4500 denier
Cost reduction
Mechanical performance

ABSTRACT

Material and processing costs are essential aspects for the further development and commercialization of all-oxide ceramic matrix composites (Ox-CMCs). Recently, progress has been made on significantly reducing the price of oxide fibers by producing rovings with higher filament counts. Thus, the objective of this work is to evaluate the effect of fabrics with higher denier on the processing and mechanical performance of Ox-CMCs. Fiber bundles and composites using fabrics with 4500 denier Nextel™ 610 rovings were characterized and compared to the classic fabric with 1500 denier. Although the fibers show similar characteristic strength, the lower denier bundles can sustain higher maximum stresses. In general, composites with higher denier show 15% lower on-axis strength and 10% lower off-axis strength. On the other hand, the use of fabrics with 4500 denier allows a fiber cost reduction of 60% and labor time reduction of 33% during critical processing steps such as lamination.

1. Introduction

Oxide fibers are used to reinforce porous matrices in all-oxide ceramic matrix composites (Ox-CMCs). The resultant composites show an interesting combination of properties such as high strength, high thermal and chemical resistance, as well as damage tolerance [1]. The overall development of this class of composites is relatively recent as the first major breakthroughs happened in the 1990s [2]. Between the current challenges for the further development and commercialization of these materials, cost reduction is of major importance. In general, the high costs of Ox-CMC components are related to their complex processing, which is often made manually, and the price of the raw materials, especially of the oxide fibers. The latter is rather significant as it can represent 70% of the price of simple Ox-CMC components [3]. Hence, it is only logical that the production of cheaper oxide fibers can lead to the overall reduction in Ox-CMCs production costs. Nevertheless, this cost reduction should be not heavily impair the mechanical properties of the fibers considering that they are the main load-bearing component of a composite.

Among the current commercially available oxide fibers, Nextel™ 610 fibers from 3 M Co. (St. Paul, MN, USA) are distinguished as having the highest tensile strength [4]. These fibers are fabricated by a spinning process based on sol gel [5]. During the extrusion of the fibers, it is easier to control fiber morphology and microstructure by extruding bundles with a relatively low filament count. In this regard, Nextel™ fibers are categorized depending on their denier, which represents the bundle weight per 9000 m. Hence, there is a clear preference for using fiber bundles with lower denier, although they are the least cost effective to produce. This can be seen as most of current high-strength Ox-CMCs use Nextel™ 610 DF11-1500-8HS fiber fabrics, which contains fiber bundles with 1500 den (the finest available) weaved in an 8 harness-satin (8HS) pattern. More recently however, it has been shown that the price of these fibers can be drastically reduced by increasing the filament count. For instance, Nextel™ 610 fiber bundles with 4500 den have a relative price of about 64% in relation to bundles with 1500 den, considering commercial prices per weight at the time of this publication. The increase in filament count leads to a change in fiber shape from cylindrical to oval [3,6]. This change in morphology is normally associated to drying

* Corresponding author.
** Corresponding author.
E-mail addresses: renato.almeida@uni-bremen.de (R.S.M. Almeida), tushtev@uni-bremen.de (K. Tushtev).

https://doi.org/10.1016/j.oceram.2023.100389
Received 29 December 2022; Received in revised form 15 May 2023; Accepted 14 June 2023
Available online 15 June 2023

conditions of bundles with higher denier, although fiber strength remains similar. Naturally, the price of the fiber fabric depends not only on the fiber production, but also on the weaving process. 3 M has introduced the Nextel™ 610 DF13-4500-5HS containing 4500 den rovings waved in a 5HS pattern. This fabric has a relative cost of 40% in relation to the standard DF11-1500-8HS, considering commercial prices per square meter at the time of this publication.

From a development point of view, cost reduction can only be effective if the trade-off with the remaining properties is not high. This seems to be the case for the new "low-cost" Nextel™ fiber fabrics from 3 M. It has been reported that composites with these new fabrics show slightly lower tensile and bending strength to standard composites with DF11-1500-8HS, although there are noticeable differences on the fiber morphology and bundle strength [6]. Nevertheless, the use of fabrics with higher denier can also affect the surface roughness of the produced composites, which is detrimental for certain applications [7]. Nonetheless, these fabrics are still relatively new and composites using them need to be further studied. Therefore, the objective of this work is to investigate the mechanical performance under several types of loadings of Ox-CMCs using the fiber fabric DF13-4500-5HS as the reinforcement. For comparison, the same procedure is conducted on composites with the fabric DF11-1500-8HS. The results are discussed not only regarding the properties of fibers and composites, but also on the processing aspects and possible cost reductions that the use of fabrics with higher denier can achieve.

2. Experimental

2.1. Materials

Nextel™ 610 fibers with 4500 den were the main object of studies. These were provided in the form of fabrics with 5 harness-satin configuration (DF13-4500-5HS), as well as fiber roving (not woven). Furthermore, the fabric DF11-1500-8HS was also investigated. A picture of both fabrics can be seen in Fig. 1 showing the thickness of the bundles as well as the different patterns and pick count. The difference in pick count is to compensate on the difference of bundle thickness. Before the characterization of the fibers or processing of the composites, all fabrics and rovings were heat cleaned following the instructions of the supplier.

Composite plates were fabricated to investigate the influence of the studied fabrics on the properties of the composites. The processing was done by press technology following the parameters based on the commercial composite Keramikblech® type FW12 [8]. For both types of composite, the same water-based slurry with organic binder was used to achieve a matrix with composition of 85 wt% of alumina and 15 wt% yttria-stabilized zirconia (3 mol%). The fiber fabrics were infiltrated with the ceramic suspension using knife blade coating. Subsequently, the infiltrated fabric layers were stacked together and pressed to the desired thickness. The green bodies were then dried at 95 °C and later sintered at 1200 °C for 5 h. The physical properties of the produced composites are listed in Table 1. It should be highlighted that, due to the higher thickness of the DF13-4500-5HS fabrics, fewer layers were necessary to achieve a similar thickness to the standard material. In addition, a slightly lower fiber content was achieved for the FW12-4500 composite.

2.2. Characterization methods

Fiber characterization was performed via fiber bundle tensile tests. For that, bundles were extracted from both warp and fill directions of the studied fiber fabrics. In addition, samples were prepared from the Nextel™ 610 roving with 4500 den as well. The tests were performed following the standard DIN EN 1007–5 using a universal testing machine Zwick/Roell Z005 (Zwick Roell Group, Ulm, Germany). Prior testing, the initial bundle cross-section area was calculated based on the sample weight and density, following the standards DIN EN 1007–2 and DIN EN 1007–5. Three samples with gauge length of 25 mm were tested per material with a loading speed of 0.1 mm/min. Acoustic emission (AE) was used to identify the failure of the fibers within the bundle during the tensile tests using an AE system AMSY4-PC equipped with two VS600-Z2 sensors (Vallen Systeme GmbH, Icking, Germany). Parameters for AE hit detection were threshold of 40 dB, duration discrimination time of 50 μs and rearm time of 100 μs. With this set-up, both fiber bundle strength and fiber failure distribution were measured. Anderson-Darling (AD) test [9] was performed to analyze whether the Weibull distribution can properly describe the fiber failure data. Further details about the fiber bundle tests with AE analysis can be seen in our previous publication [10].

The produced composites were characterized regarding their microstructure and mechanical properties. Mercury porosimetry was conducted with a porosimeter Pascal 140 and 440 (Porotec GmbH, Hofheim am Taunus, Germany) using mercury surface tension of 480 Dyne/cm and contact angle of 141.3°. Furthermore, micrographs of the composite microstructures were taken with a scanning electron microscope (SEM) model Camscan Series 2 (Obducat CamScan Ltd., Waterbeach, United Kingdom). For that, composite samples were sectioned and embedded in epoxy resin for gridding and polishing of their cross-section. Mechanical characterization of the composites was performed under several loading conditions. Composite strength was measured by tensile test (DIN EN 658–1), compression test (DIN EN 658–2) and four-point bending test (DIN EN 658–3). Fracture toughness in terms of critical stress intensity factor (K_{IC}) was analyzed by single-edge notch bending test (DIN 51 109). In-plane shear strength was measured by Iosipescu shear test (DIN EN 12289), while interlaminar shear strength was measured by short-beam bending tests (DIN EN 658–5). For all tests, a total of three samples per material were tested with a traveling speed of 1 mm/min. Both tensile and compression tests were performed on a universal testing machine Zwick 1465 (Zwick Roell Group, Ulm, Germany) equipped with a multi-axis extensometer 632.85F-05 (MTS Systems Corporation, Eden Prairie, MN, USA), while the other tests were

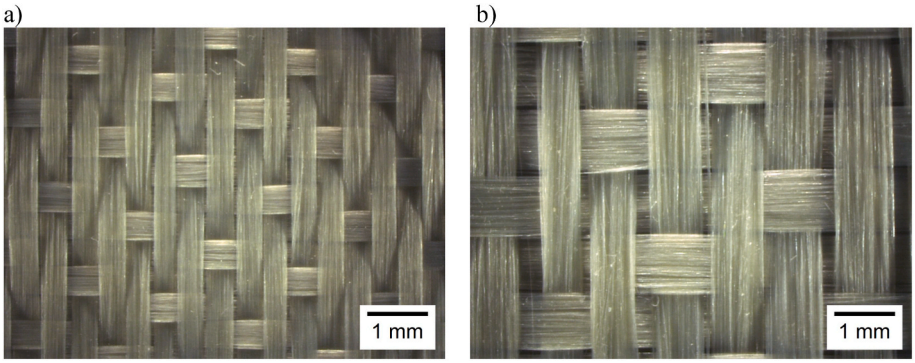

Fig. 1. Investigated Nextel™ 610 fiber fabrics: DF11-1500-8HS (a) and DF13-4500-5HS (b).

Table 1
Physical properties of studied composites.

Composite	Matrix	Fabric type	Nominal filament count (filaments per tow)	Fabric thread count (rovings per cm)	Number of fabric layers	Average composite thickness (mm)	Fiber content (%)	Total porosity (%)
FW12-1500	85% Al_2O_3 + 15% 3YSZ	DF11-1500-8HS	400	11	12	2.9	39.9	27.8
FW12-4500	85% Al_2O_3 + 15% 3YSZ	DF13-4500-5HS	1125	4.7	8	2.6	37.5	31.0

performed using the same testing machine used for the fiber bundle tests. Tensile tests were performed in two directions in relation to the fiber orientation: on axis (0°/90°) and off axis (±45°). In both cases, dog-bone shaped specimens were used. It should be noted that due to the width of the fiber bundles of the DF13-4500-5HS fabric, tensile specimen samples of FW12-4500 had a bigger width of 15 mm in the reduced section in comparison to FW12-1500 samples with width of 10 mm. The dimensions of the samples for the other tests were kept the same for a direct comparison and to be in accordance to the respective standards. After the tests, the fracture surfaces of the samples were observed using a digital light microscope VHX-6000 (Keyence Deutschland GmbH, Neu-Isenburg, Germany).

3. Results

3.1. Fiber characterization

Fiber bundles extracted from the studied fabrics, as well as directly from the Nextel™ 610 4500 den roving, were tested to evaluate the effect of filament count and weaving process on fiber properties. Examples of stress-strain curves measured during the bundle tensile tests are displayed in Fig. 2a. Although differences are perceivable between the different materials, the shapes of the curves are rather similar. For all samples, there is an initial non-linear part, in which the fibers are tensioned and aligned together, followed by a linear-elastic part. As the fibers start to fail, the inclination of the curve starts to decrease. At the same time, AE activity starts to increase. The fibers of the bundle progressively fail until reaching the maximum apparent stress. After the maximum stress, the bundle loses its integrity and the load slowly decreases towards zero. In some cases, it is observed that the load does not reach zero due to friction between the broken fibers. The main difference between the samples with different denier lies on the bundle apparent strength, calculated as the maximum force divided by the initial cross section of the bundle (see Table 2). Fiber bundles with 1500 den show higher bundle strength in comparison to 4500 den. In general, the stress-strain curve of 4500 den samples is more flattened, showing lower maximum stress but higher maximum strain. Furthermore, the weaving process also seems to have an effect on the maximum stress as the samples from the roving show higher bundle strength than samples extracted from both directions of the fabric. Also in this regard, fill samples show slightly lower bundle strength than warp samples.

AE data was used to identify the failure of the fibers in the bundle during the tensile tests and measure the failure distribution following the Weibull distribution as shown in Fig. 2b. The parameters that describe the distributions are given in Table 2. Contrary to the fiber bundle apparent strength, fiber characteristic strength is rather similar for all samples. Nevertheless, differences are seen in the shape of the distribution and Weibull modulus. In general, fiber bundles with 1500 den show higher Weibull modulus, but there is no noticeable trend regarding fiber direction. Furthermore, it can be seen that the shape of the distribution for fiber bundles with 4500 den diverges from a line in the logarithmic plot of Fig. 2b. This is an indication that the data deviates from the Weibull distribution. AD test was performed to measure

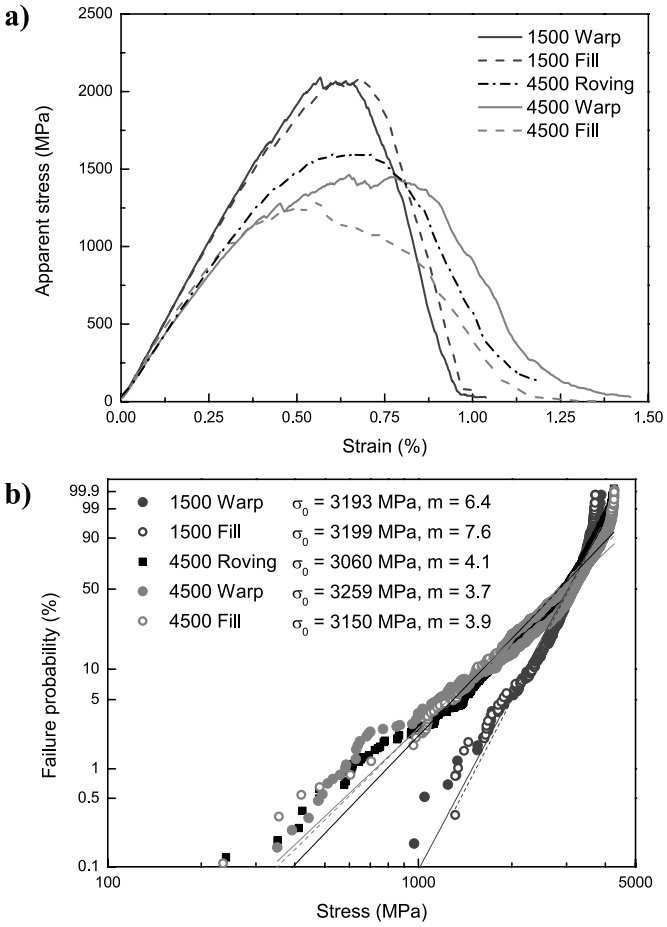

Fig. 2. Examples of stress-strain curves from fiber bundle tensile on bundle extracted from the studied fabrics and unwoven 4500 den roving (a). Stress values are calculated considering the initial bundle cross-section. Weibull distribution of fiber strength of the respective fiber bundle tests (b).

the goodness of the fit for all distributions. As seen in Table 2, AD values are higher for the samples with 4500 den, indicating higher deviation from the Weibull distribution.

3.2. Composite characterization

The composites produced with the investigated fiber fabrics were characterized regarding their microstructure and mechanical properties. Fig. 3 shows the microstructure of both composites. As previously mentioned, the fabrics with 4500 den show different fiber morphology, in which 60% of the fibers have an elliptical cross-section, while the remaining fibers are round. Despite the different shape, both fiber types have very similar cross-section area of 104.9 ± 4.9 μm^2 and 108.6 ± 4.8 μm^2 for oval and cylindrical fibers, respective. In contrast, all fibers in

Table 2
Results obtained from fiber bundle tests of samples extracted from fill and warp direction of studied fiber fabrics and from unwoven 4500 den roving.

Bundle sample	Apparent strength (MPa)	Characteristic strength (MPa)	Weibull modulus	Anderson-Darling test
1500-8HS Warp	2000 ± 102	3193	6.4	2.7
1500-8HS Fill	1839 ± 200	3199	7.6	2.9
4500 Roving	1647 ± 48	3060	4.1	8.4
4500-5HS Warp	1543 ± 73	3259	3.7	12.6
4500-5HS Fill	1423 ± 61	3150	3.9	6.9

the 1500 fabric are round, having an average cross-section area of 106.6 ± 4.6 μm^2. The matrix-rich region between the fabric layers is rather similar. In both cases, defects like shrinkage cracks and pores are occasionally observed along the matrix, which is typical for this type of composite [11]. Nevertheless, FW12-4500 composite shows a higher amount of intra-bundle defects, which are the dark spots between the fibers in the micrographs seen in the lower magnification micrographs of Fig. 2.

The total porosities of the composites are slightly different with FW12-1500 having 27.8% porosity, while FW12-4500 has 31.0% porosity (see Table 1). The pore size distributions of the studied composites are given in Fig. 4. Most pores are either in the range of 0.1 μm or 1 μm. These small pores are a result of the relatively low sintering temperature. It should be highlighted that the presence of small pores is essential for damage tolerance since they are responsible for enabling crack deflection mechanisms [2]. On the other hand, the pores in the range of 10 μm or higher are related to processing defects. As seen in the micrographs from Fig. 3, pores of about 10 μm are observed in the fiber bundle regions, while bigger pores are observed in the matrix-rich region. In this regard, although FW12-1500 shows more pores in the range of 1 μm, FW12-4500 shows more pores above 10 μm. As a result, the average pore size of FW12-4500, 143 nm, is bigger than FW12-1500, 123 nm.

The mechanical properties of the composites were evaluated under various types of mechanical loadings. To exemplify their mechanical performance, Fig. 5a shows stress-strain curves of tensile tests on both 0°/90° and ±45° orientations. When loaded in the same direction as one of the fiber axes, the composites show mostly linear-elastic deformation. Nevertheless, non-linear deformation is observed above 50 MPa. At this stress, the matrix probably starts to crack. Still, since most of the load is sustained by the fibers, only small changes in the overall stiffness of the composite is observed until failure. In contrast, the composites show mostly non-linear deformation when loaded off axis. In this case, the matrix sustains considerable part of the load since none of the fibers are in the same direction as the load. Therefore, the early failure of the matrix results in decrease of stiffness and strength. Overall, both composites types show very similar stress-strain response on all different types of loadings. The same can be said for their fracture surface after tensile loading, depicted in the front view micrographs of Fig. 5b and c. Although there is little non-linear deformation observed during the tensile tests at 0°/90°, they clearly fail in a non-brittle matter. In other words, the crack paths can be seen in different planes and fiber pullout is observed along the fracture surface. For the ±45°, the failure is parallel to the fiber orientation showing signals of delamination and fiber scissoring. Differences on fracture behavior were only seen for the compression tests. The side view micrographs of samples after compression tests are seen in Fig. 5d. In this case, much more interlaminar failure is observed on the fracture of the FW12-1500 composite.

The results of the mechanical tests are summarized in Fig. 6 and Table 3. Both composites show relatively high strength, reaching tensile strengths of 220–260 MPa. In general, FW12-4500 composite shows mostly lower values. Strength differences are of 14% for 0°/90° tension, 9% for ±45° tension, 14% for compression, 12% for bending, 22% for in-plane shear and 11% for interlaminar shear. When comparing the

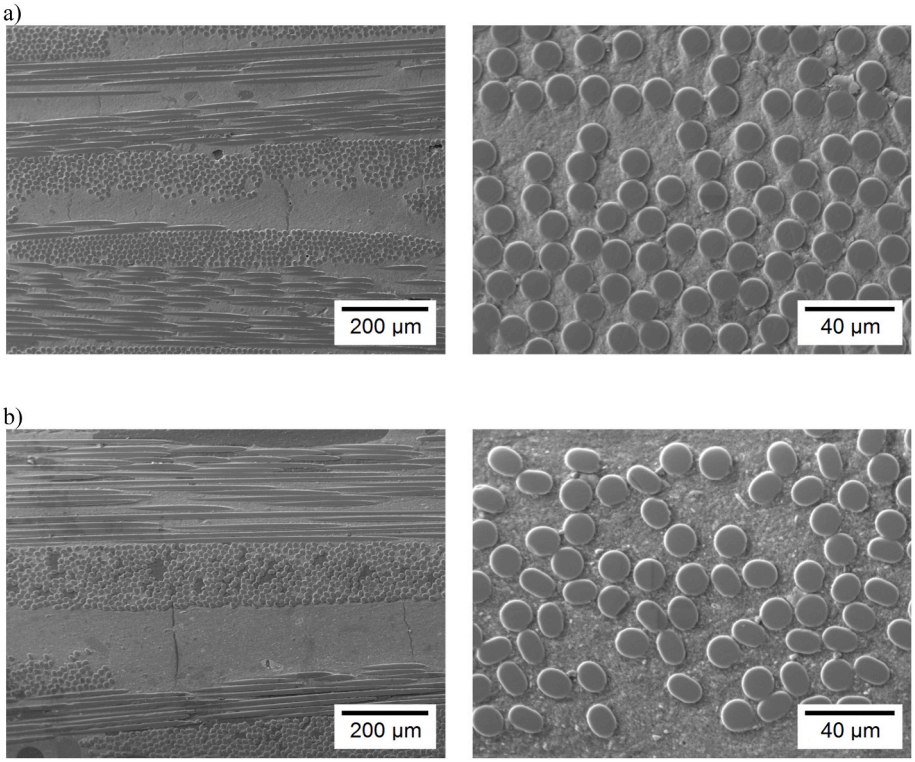

Fig. 3. Microstructure of the investigated composites: FW12-1500 (a) and FW12-4500 (b).

a)

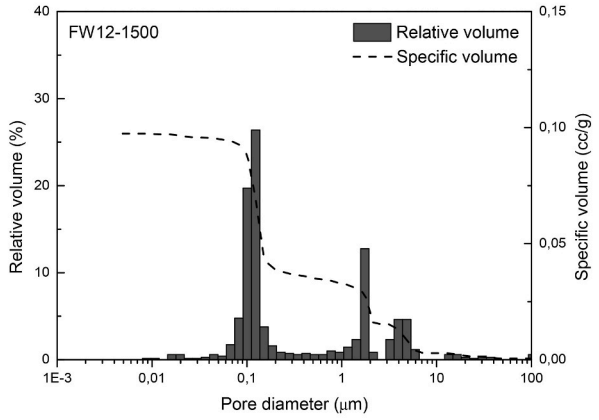

b)

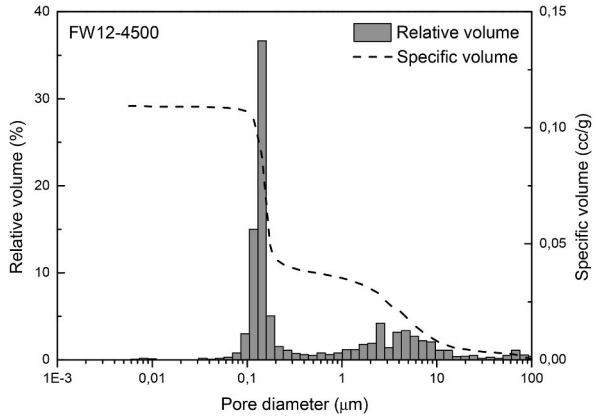

Fig. 4. Pore size distribution of the investigated composites: FW12-1500 (a) and FW12-4500 (b).

elastic modulus of the composites, differences are smaller and only for tension 0°/90° (5%) and in-plane shear (15%). Differences are also seen for the measured K_{IC} (Table 3), in which FW12-4500 shows 8% lower critical stress intensity factor. In summary, the measured differences depend on the type of loading.

4. Discussion

4.1. Mechanical performance

Ox-CMCs are normally composed of porous oxide matrices reinforced by stiff oxide fibers. Therefore, their mechanical performance is mostly dependent on the reinforcing fibers, especially when the load is applied in their direction. Hence the importance to properly characterize the fibers of the fabrics. As seen in Table 2, all fiber samples showed very similar fiber characteristic strength, but there are clear differences regarding fiber bundle apparent strength and Weibull modulus. While the characteristic strength represents the strength of fibers in the bundle following the Weibull distribution, the fiber bundle strength is the maximum apparent stress that the bundle can support before losing its integrity. In other words, bundle strength depends on the strength of the fibers of the bundles, their alignment, possible fiber interactions and friction, as well as how the load is distributed when the fibers start to fail. In this regard, although the fibers of both fabric types have similar strength, the mechanical performance when the whole bundles are loaded is different. These differences can be better understood when analyzing the fiber failure distributions (Fig. 2b). Bundles with 4500 den show a much broader distribution and lower Weibull modulus. The dispersion of fiber strength values within the fibers of a bundle is normally related to the different defect populations of each fiber. It can be expected that the individual fibers have a relatively narrow flaw size distribution. However, some fibers have a population of larger processing defects while others have smaller processing defects [12]. Hence, the overall defect distribution within a fiber bundle is broad. It should also be highlighted that most of these flaws are associated with surface defects originated during fiber processing [13,14]. As seen in Fig. 3b, fiber bundles with 4500 den contain both circular and elliptical fibers. Hence, it is safe to assume that these two types of fibers have very distinct defect size distributions, leading to a broader fiber failure distribution. The filament count can also have an effect on the measured distribution. Statistically speaking, there is a higher probability of "finding" fibers with critical defect sizes, i.e. low strength, when testing a bundle with 4500 den than testing a bundle with 1500 den. In contrast, there is also a higher chance of having almost defect-free fibers with higher strength, leading to a more disperse distribution. The presence of weaker fibers can drastically change the overall mechanical behavior of a fiber bundle (see Fig. 2a). Since the weaker fibers fail at lower stresses, the remaining fibers will be overloaded at earlier stages. The load-redistribution capability of the fibers is therefore very important since the failure of the weaker fibers can cause the premature failure of the surrounding fibers. In this regard, it should be highlighted that load-redistribution capability of fiber bundles is normally less efficient with higher filament count [6]. This can be confirmed by analyzing the AD test value. Bundles with 4500 den show higher AD value, meaning a higher deviation from the Weibull distribution. This is an indication that other factors can influence the failure of the fibers [15]; in this case, the interaction between the fibers.

Differences are also perceived when comparing the bundle strength of samples with the same denier but from different directions of the fabric or from the unwoven roving. It should be noted that for these cases, there is no significant difference between the failure distributions (Fig. 2b). It is therefore suggested that the weaving process can damage and break some of the fibers from the bundle. As the initial number of load-bearing fibers decreases, a lower apparent bundle strength is measured for the bundles of the fabric in relation to the unwoven roving. Still, since these fibers are not detected during AE analysis, the fiber failure distributions remain similar. This also helps explain why fill bundles show slightly lower results than warp bundles. Fill fiber rovings can be more damaged since there are higher stresses applied to them during the weaving process [16].

Both fiber characteristic strength and fiber bundle apparent strength can have a direct influence on the mechanical properties of the composites. As seen in Fig. 6a, FW12-4500 composite shows overall lower strength. Nevertheless, the measured differences are not so high as the differences in fiber bundle apparent strength. For instance, comparing samples with 1500 den and 4500 den, there is a difference of about 23% for both warp and fill directions (Table 2). However, this is not translated to the properties of the composites, probably because of how the fibers are distributed and sustain load in a composite. Differently from a fiber bundle, in which the fibers are lose and align to the direction of the load, embedded fibers are surrounded by matrix. Hence, even during on-axis tensile loading, the fibers will not be completely aligned to the applied load due to the natural undulation of the fiber fabrics. In addition, the difference between stiffness of fibers and matrix means that the deformation of fibers will be influenced by the deformation of matrix. Therefore, it can be expected that the failure distribution and possible interactions between fibers will be different when the whole composite is tested. As the weaker fibers fail, different damage mechanisms can release mechanical energy such as matrix cracking, fiber debonding and fiber pullout [2]. In this regard, clear signs of fiber pullout are seen in the fracture surfaces from Fig. 5b and c. Hence, load redistribution is more efficient since the failure of the weaker fibers and fiber interactions will not necessarily have such a high impact on the failure of the remaining

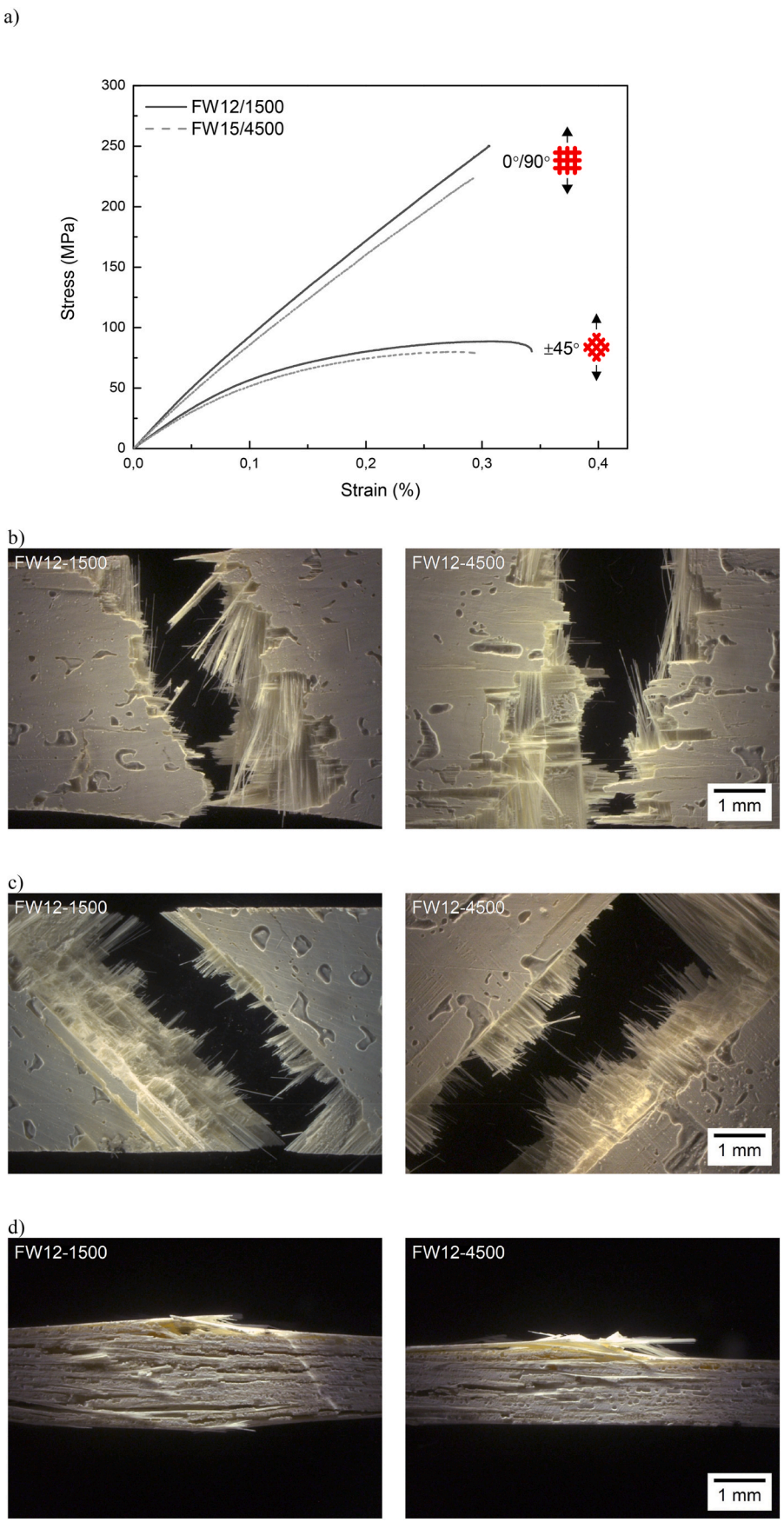

Fig. 5. Examples of stress-strain curves from composite tensile test (a). Fracture surface of samples tested under tension 0°/90° (b), ±45° (c) and compression 0°/90° (d).

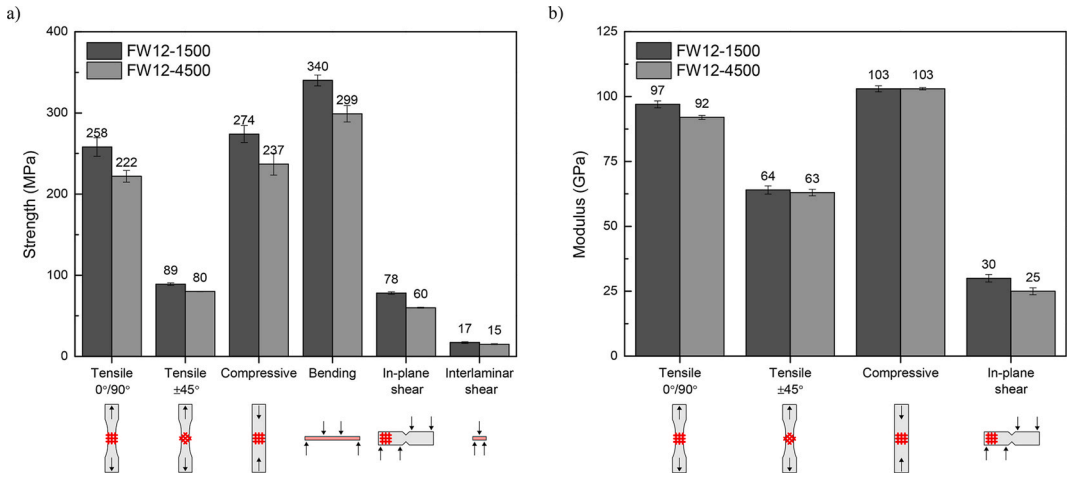

Fig. 6. Strength (a) and elastic modulus (b) of studied composites under different mechanical loadings.

Table 3
Mechanical properties of studied composites.

Property	FW12-1500	FW12-4500
Tensile strength 0°/90° (MPa)	257 ± 11	222 ± 7
Tensile strength ±45° (MPa)	88 ± 2	80 ± 1
Elastic modulus 0°/90° (GPa)	97.0 ± 1.3	92.2 ± 0.8
Elastic modulus ±45° (GPa)	64.4 ± 1.6	62.6 ± 1.2
Compressive strength (MPa)	274 ± 10	237 ± 13
Compressive modulus (GPa)	103.4 ± 1.1	102.6 ± 0.4
Bending strength (MPa)	340 ± 7	300 ± 10
K_{IC} (MPa*$m^{1/2}$)	14.7 ± 0.4	13.5 ± 0.6
In-plane shear strength (MPa)	78 ± 2	60 ± 1
Shear modulus (GPa)	30.3 ± 1.4	25.8 ± 1.3
Interlaminar shear strength (MPa)	17 ± 1.1	15 ± 0.6

fibers as seen for the fiber bundle tests (Fig. 2a).

Differences between the composites with different fabrics also depend on the type of loading. From the experiments performed, the measured properties can be divided into on or off axis. On-axis properties such as 0°/90° tensile, compression, bending and in-plane shear strength showed higher discrepancy between the studied composites reaching differences of about 15% for most cases. These properties are mainly dependent on the strength of the fibers and microstructural features such as fiber volume content and porosity. Here it should be highlighted that the FW12-4500 composite shows slightly lower fiber volume content and higher porosity (see Table 1). Furthermore, the geometry of the fabrics can also influence mechanical performance such as the behavior during compressive tests. Failure under compression of Ox-CMCs is generally caused by local fiber damage and fiber bundle buckling [17]. Therefore, the thickness of the fiber bundle and pattern of the fabric can influence the failure. In this sense, the lower undulation of DF11-1500-8HS fabrics makes the fabric layers stronger under compression in comparison to the thicker DF13-4500-5HS fabrics. As a result, cracks arise mostly on the interlaminar region (see Fig. 5d). The strength of the composite under other loading conditions may not be dependent on the weave architecutre however. In our previous study [6], no differences in bending strength were observed for composites containing Nextel™ fabrics with 4500 den tows and 8HS and 5HS configuration, althoguh the composite with 5HS configuration showed slightly higher tensile strength. Still, an actual tendency relating fabric configuration and tensile or bending strength was not observed when considering other configurations such as 4HS and 2x2 twill.

Off-axis properties such as ±45° tensile strength showed lower differences of about 10% between the composites. In such cases, the matrix plays a bigger role since the fibers are not in the main direction of the load. Therefore, matrix properties and the presence of microstructural defects can influence the measured values of strength. As seen in the micrographs of Fig. 3, FW12-4500 composite shows more intra-bundle defects. These defects appear on the regions were the fibers are highly compacted. Therefore, they are probably related to problems during the infiltration process and can influence the off-axis behavior. Other properties such as elastic moduli and K_{IC} seem to be less influenced by the used fabrics in this study. The elastic moduli depend mainly on the stiffness of both fibers and matrix, their respective volume content and the direction of the load. As for K_{IC}, it will depend not only on the fiber reinforcement, but also on toughening mechanisms such as crack deflection and interactions between fibers and matrix [18].

4.2. Processing aspects

Besides the mechanical properties, another very important aspect to be discussed is the influence of fabrics with higher denier on the processing of the composites. The use of DF13-4500-5HS can affect not only material costs, but also important processing steps such as infiltration and shaping. In general, thicker bundles and fabrics are normally more difficult to infiltrate. Nonetheless, it was noted that both fabrics behaved similarly during the infiltration step. The rovings that form the fabric DF13-4500-5HS are more spread than the ones from DF11-1500-8HS. It was also noted that there is more space between the rovings of the fabric DF13-4500-5HS, which might be the cause for the slightly lower fiber volume content (see Table 1). Furthermore, DF13-4500-5HS has a lower pick count to account for differences in bundle width, as seen in Fig. 1. As a result, the new fabric is somewhat looser than the standard DF11-1500-8HS and is slightly easier to work with. Still, intra-bundle defects are seen on the regions where the fibers are highly compacted (Fig. 3b), while no defects are seen where the fibers are more dispersed (see higher magnification micrograph from Fig. 3b). In this regard, the use of slurries with lower viscosity can help obtain a more homogenous microstructure, for example. Although not investigated in this study, it is also expected that the production of components with small radius to be more difficult when working with fabrics such as the DF13-4500-5HS. This is because of its thicker bundles and lower pick count. Nevertheless, first experiments have shown that components with complex shapes can be indeed produced with this fabric type.

The biggest advantage of using fabrics with higher denier is cost reduction. As aforementioned, the price of DF13-4500-5HS fabric is 40% relative to the price of DF11-1500-8HS. Naturally, there are other costs related to the production of composites such as the raw materials for the matrix and the processing itself. Yet, these costs are much smaller than fiber costs. For instance, matrix and processing together account for around 15% of the total costs of the studied FW12-1500 composite. Energy costs are not considered above since they are relatively small for

pressing technique. However, they can have a higher influence on more complex processing techniques. Moreover, the use of thicker fabrics can also promote cost reduction in other steps of the processing. For the production of Ox-CMCs reinforced with fiber fabrics, each fabric layer is normally infiltrated, stacked and shaped to obtain the desired component thickness. In many cases, this procedure is done manually, representing a critical step in processing. Therefore, the use of thicker fabrics can lead to a significant reduction in labor time as fewer fabric layers are needed to achieve the same component thickness. In the example of this study, FW12-4500 consisted of 8 layers of DF13-4500-5HS, while FW12-1500 consisted of 12 layers of DF11-1500-8HS. This represents a reduction in the labor time during the whole lamination process of up to 33%. Although there is a trade-off between cost efficiency and mechanical performance, the aforementioned loss in strength is much smaller than these cost reduction possibilities. It should also be highlighted that the studied composites still show high mechanical performance. For instance, reported tensile strength values of Ox-CMCs using Nextel™ 610 are typically in the range of 150–300 MPa [1]. Therefore, the strength of 222 ± 7 MPa of the studied FW12-4500 composite is relatively high.

5. Conclusions

In this work, the mechanical performance of Ox-CMCs produced with the "low-cost" Nextel™ 610 DF13-4500-5HS fabric were evaluated and compared to the standard DF11-1500-8HS. The analyses included the characterization of fiber bundles extracted from these fabrics, as well as composites reinforced by them. Fiber characterization showed that both types of fabrics have similar fiber characteristic strength, but different bundle apparent strength. This is associated with the broader fiber failure distribution of bundles with higher denier. Altogether, the presence of different fiber shapes, higher filament count and possible interactions between the fibers can change the mechanical behavior of the whole fiber bundle at earlier stages of loading. Hence, bundles with 4500 den show 23% lower fiber bundle apparent strength. Furthermore, differences are seen between bundles extracted from the different weaving directions and unwoven roving. This is probably because fibers are damaged during the weaving process, therefore leading to fewer load-bearing fibers during the bundle tests.

In general, FW12-4500 composite show high strength under different types of mechanical loading. Nevertheless, the results are lower than the ones from the standard FW12-1500 composite. When the mechanical load is applied in the direction of the reinforcing fibers, differences of about 15% in strength are observed. For off-axis properties, differences of about 10% are measured. It is suggested that these properties depend on the strength of the fibers, fiber volume content and the presence of intra-bundle defects. Nevertheless, the main benefit of DF13-4500-5HS is related to cost efficiency. The use of this lower-cost fabric can represent up to 60% reduction on costs of raw materials. In addition, the higher thickness of the fabric means that fewer layers are necessary to obtain the desired component thickness. Thus leading to a reduction of 33% on labor-intense processing steps such as fiber infiltration, stacking and shaping of Ox-CMCs. In summary, there is a trade-off between mechanical properties and fiber cost. Nevertheless, the loss in mechanical performance can be compensated by the gain in cost efficiency depending on the application. This is a very important aspect since cost reduction can broaden the possible fields of application of Ox-CMCs. In addition, the use of cheaper materials can also benefit the overall development of these composites as more processing parameters and materials properties can be evaluated for a lower cost.

Declaration of cometing interest

The authors declare that they have no known competing financial interests or personal relationships that could have appeared to influence the work reported in this paper.

Acknowledgments

The authors express their gratitude to A. Trajano and M. Martin for the help with the mechanical tests. This research did not receive any specific grant from funding agencies in the public, commercial, or not-for-profit sectors.

References

[1] K. Tushtev, R.S.M. Almeida, Oxide/oxide CMCs – porous matrix composite systems; Composites with interface coatings, in: P.W.R. Beaumont, C.H. Zweben (Eds.), Comprehensive Composite Materials II, Elsevier, Oxford, 2018, pp. 130–157.
[2] F.W. Zok, Developments in oxide fiber composites, J. Am. Ceram. Soc. 89 (11) (2006) 3309–3324.
[3] J. Lincoln, B. Jackson, A. Barnes, A.R. Beaber, L. Visser, Oxide-oxide ceramic matrix composites - enabling widespread industry adoption, Ceram. Trans. 263 (2018) 401–412.
[4] B. Clauß, Fibers for ceramic matrix composites, in: W. Krenkel (Ed.), Ceramic Matrix Composites, Wiley-VCH Verlag GmbH & Co. KGaA, 2008, pp. 1–20.
[5] D.M. Wilson, Spun (slurry and sol-gel) ceramic fibers, in: S. Hashmi (Ed.), Reference Module in Materials Science and Materials Engineering, Elsevier, 2016, pp. 8779–8782.
[6] W.E.C. Pritzkow, R.S.M. Almeida, L.B. Mateus, K. Tushtev, K. Rezwan, All-oxide ceramic matrix composites (OCMC) based on low cost 3M Nextel™ 610 fabrics, J. Eur. Ceram. Soc. 41 (5) (2021) 3177–3187.
[7] A. Tontisakis, W. Simpson, J. Lincoln, R. Dhawan, M. Opliger, Evaluation of surface finish technology in the manufacture of Oxide-Oxide ceramic matrix composites, Ceram. Int. 47 (4) (2021) 5347–5363.
[8] W.E.C. Pritzkow Spezialkeramik, Oxide/oxide Ceramic Matrix Composite Keramikblech®, 2012. https://www.keramikblech.com/fileadmin/user_upload/pdf/New_materials.pdf (accessed 1 Decenber 2022).
[9] N.M. Razali, Y.B. Wah, Power comparisons of shapiro-wilk, Kolmogorov-smirnov, lilliefors and anderson-darling tests, Journal of Statistical Modeling and Analytics 2 (1) (2011) 21–33.
[10] R.S.M. Almeida, E.L. Bergmüller, B.G.F. Eggert, K. Tushtev, T. Schumacher, H. Lührs, B. Clauß, G. Grathwohl, K. Rezwan, Thermal exposure effects on the strength and microstructure of a novel mullite fiber, J. Am. Ceram. Soc. 99 (5) (2016) 1709–1716.
[11] P.O. Guglielmi, D. Blaese, M.P. Hablitzel, G.F. Nunes, V.R. Lauth, D. Hotza, H.A. Al-Qureshi, R. Janssen, Microstructure and flexural properties of multilayered fiber-reinforced oxide composites fabricated by a novel lamination route, Ceram. Int. 41 (6) (2015) 7836–7846.
[12] D. Wilson, Statistical tensile strength of Nextel™ 610 and Nextel™ 720 fibres, J. Mater. Sci. 32 (10) (1997) 2535–2542.
[13] P.E. Cantonwine, Strength of thermally exposed alumina fibers – Part I. Single filament behavior, J. Mater. Sci. 38 (3) (2003) 461–470.
[14] P.E. Cantonwine, Strength of thermally exposed alumina fibers – Part II. Bundle behavior, J. Mater. Sci. 38 (3) (2003) 471–480.
[15] R. Danzer, P. Supancic, J. Pascual, T. Lube, Fracture statistics of ceramics – Weibull statistics and deviations from Weibull statistics, Eng. Fract. Mech. 74 (18) (2007) 2919–2932.
[16] F. Boussu, C. Dufour, F. Veyet, M. Lefebvre, Weaving processes for composites manufacture, in: P. Boisse (Ed.), Advances in Composites Manufacturing and Process Design, Woodhead Publishing, 2015, pp. 55–78.
[17] D. Koch, K. Tushtev, G. Grathwohl, Ceramic fiber composites: experimental analysis and modeling of mechanical properties, Compos. Sci. Technol. 68 (5) (2008) 1165–1172.
[18] J.A. Heathcote, X.Y. Gong, J.Y. Yang, U. Ramamurty, F.W. Zok, In-plane mechanical properties of an all-oxide ceramic composite, J. Am. Ceram. Soc. 82 (10) (1999) 2721–2730.